

# Size-dependent shock response mechanisms in stacked nanoparticles of 1,3,5-triamino-2,4,6-trinitrobenzene

*Guanchen Dong<sup>a, b</sup>, Jialu Guan<sup>a, b</sup>, Jing Lv<sup>a, b</sup>,  
Linghua Tan<sup>a, b, \*</sup>, Xiaona Huang<sup>c, \*</sup>, Guangcheng Yang<sup>a, d, \*</sup>*

- a** School of Chemical Engineering, Nanjing University of Science and Technology, Nanjing, 210094, China.
- b** National Special Superfine Powder Engineering Research Center, Nanjing University of Science and Technology, Nanjing 210094, China.
- c** College of Power and Mechanical Engineering, Wuhan University, Wuhan, 430072, China.
- d** China Academy of Engineering Physics·Institute of Chemical Materials, Mianyang, 621900, China.

**SUPPORTING INFORMATION**

## Energy curves during relaxation after compression

Since the compression were conducted under the NVE ensemble at 300K, Figs. S1 a, c, and e indicate no significant energy change during relaxation, suggesting that the configurations generated by the compression simulation are physically reasonable. Furthermore, the convergence of the energy curves in Fig. S1 confirms that the configurations used for the shock simulations have undergone sufficient relaxation.

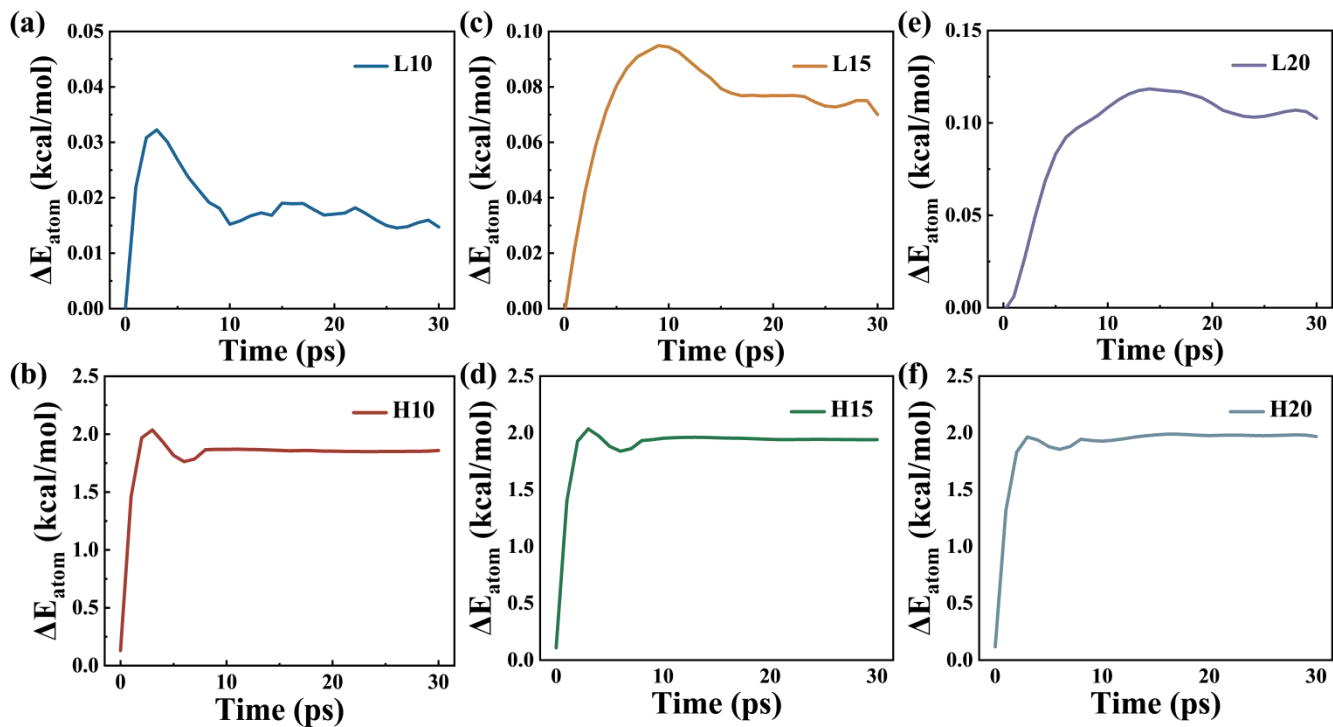


Fig. S1. Relaxation energy curves of compressed nanoparticle TATB configurations after removing noise: particle size is (a), (b) 10 nm, (c), (d) 15 nm, and (e), (f) 20 nm. 'L' denotes an initial temperature of 300K, while 'H' denotes 600K.  $\Delta E_{\text{atom}}$  indicates the increase in the average energy per atom over that of the initial compressed configuration.

## Structural features and mechanical properties

The radial distribution functions (RDF) of uncompressed TATB nanoparticles and equilibrated simulation configurations are shown in Fig. S2a, and Fig. S2b presents the stress – strain curves under uniaxial compression.

Smaller particles exhibit a more ordered molecular arrangement, which enhances their structural integrity and leads to a higher densification threshold. In contrast, elevated initial temperatures introduce greater structural disorder and make void elimination, thereby increasing the available free volume and significantly reducing the densification threshold.

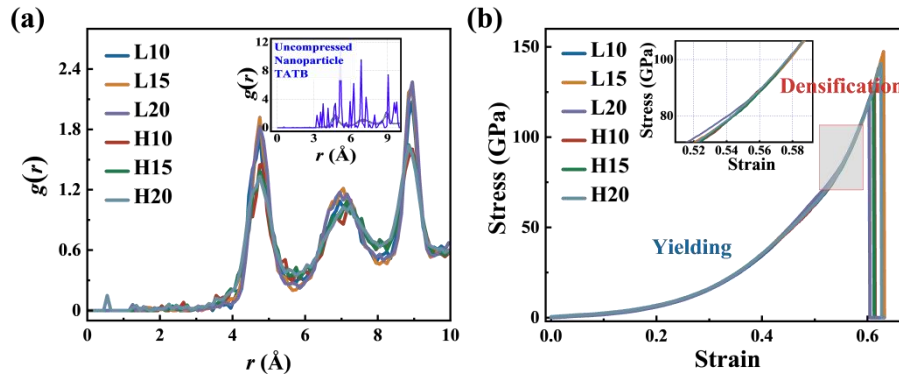


Fig. S2. (a) Molecular radial distribution function, and (b) stress-strain curve under z-axis compression in the simulation configurations. "L" denotes low initial temperature (300 K), "H" denotes elevated initial temperature (600 K), and the following numbers represent particle size.

### Temperature distribution functions at different time

At lower initial temperatures, larger particles exhibit a stronger tendency for temperature localization, reflecting the influence of void collapse and structural ordering. In contrast, at higher initial temperatures, the effect of particle size becomes less pronounced, and the temperature distribution shows no significant dependence on particle size.

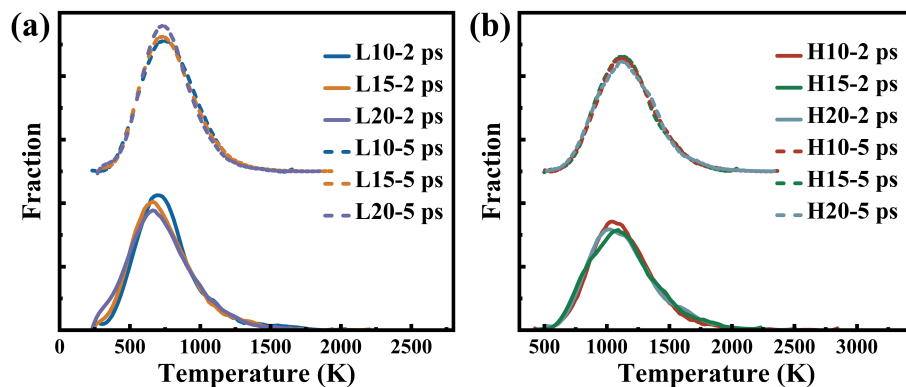


Fig. S3. Temperature distribution functions for shocked TATB molecular within different particle size configurations at 2 and 5 ps under shock loading with initial temperatures of (a) 300 K and (b) 600 K.

## PE-temperature plots for 15, 20 nm configurations

Fig. 6 in the main text and Fig. S4 show that the PE-T do not differ significantly in particle size.

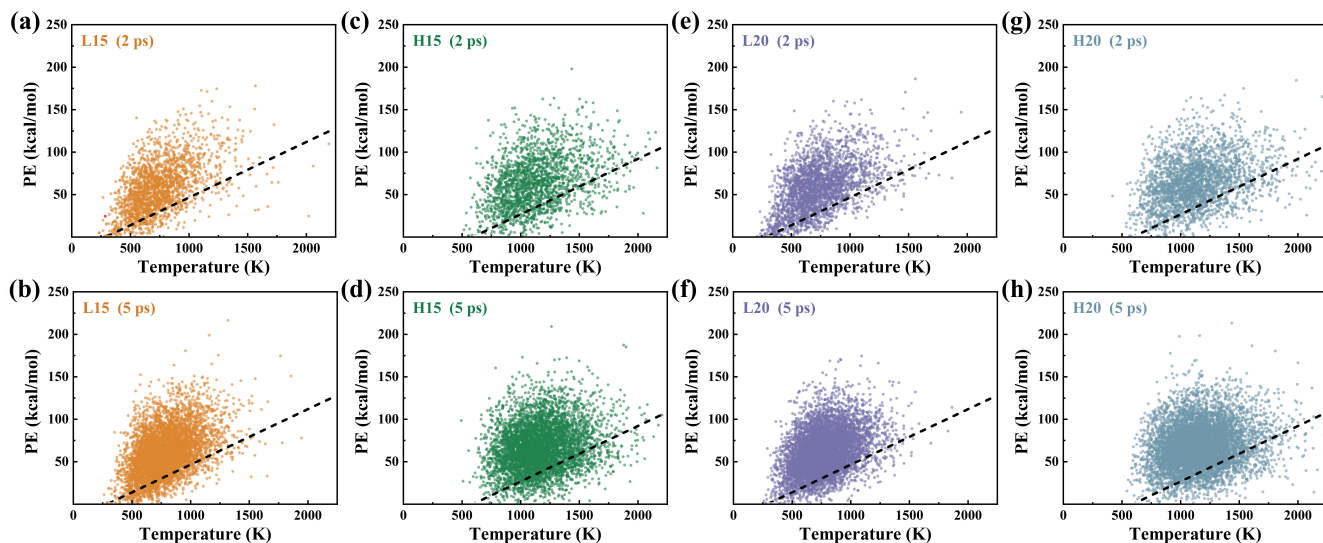


Fig. S4. PE-temperature plots for 10, 15, 20 nm configurations in different initial temperatures (a), (c), (e), and (g) at 2 ps and (b), (d), (f), and (h) at 5 ps, where PE is the rise in intramolecular potential energy from the unshocked state. The labels on each plot designate the initial temperature and particle size. Dashed lines represent classical equipartition of energy.